THE ASTROPHYSICAL JOURNAL, 461:600–608, 1996 April 20

EQUIPARTITION DOPPLER FACTORS FOR A SAMPLE OF ACTIVE GALACTIC NUCLEI

ALBERTO GÜIJOSA AND RUTH A. DALY[1]
Department of Physics, Joseph Henry Laboratories, Princeton University, NJ 08544
Received 1995 July 13; accepted 1995 October 20

ABSTRACT

The Doppler factor of the outflow from compact radio cores of active galactic nuclei (AGNs) can be estimated from single-epoch radio observations by assuming that the particles and magnetic field are in equipartition, as suggested by Readhead. This estimate of the Doppler factor is called the equipartition Doppler factor, δ_{eq}. To test whether δ_{eq} is a good estimator of the true Doppler factor, equipartition Doppler factors are computed for a sample of 105 radio sources and compared with the corresponding inverse Compton (self-Compton) Doppler factors, δ_{IC}, computed for this same sample by Ghisellini and coworkers, by assuming the observed X-ray flux to be of inverse Compton origin.

The Ghisellini et al. sample consists of 33 BL Lacertae objects, 24 core-dominated high-polarization quasars, 29 core-dominated low-polarization quasars (including seven core-dominated quasars with no polarization data), 11 lobe-dominated quasars, and eight radio galaxies. The relevant assumptions for the computation of both the equipartition Doppler factor, δ_{eq}, and the inverse Compton Doppler factor, δ_{IC}, are discussed. A high correlation is found between these two estimates of the true Doppler factor, suggesting that they are both reliable. In fact, it appears that δ_{eq}/δ_{IC} is on the order of unity. This seems to indicate that the sources are near equipartition, and thus confirms the possibility of using δ_{eq} to estimate the true Doppler factor of a source from single-epoch radio data.

It appears that the Doppler factors of radio galaxies and lobe-dominated quasars are lower than those of the other categories of sources. This may be related to orientation effects, and could therefore be used to constrain orientation unified models. In any case, equipartition Doppler factors are likely to play a crucial role in our understanding of the physics at work in compact radio sources

Subject headings: BL Lacertae objects: general — galaxies: active — galaxies: kinematics and dynamics — quasars: general — radiation mechanisms: nonthermal — radio continuum: galaxies — relativity

1. INTRODUCTION

One of the many interesting problems of current extragalactic research is the determination of the physical processes that occur in the compact radio emission regions of active galactic nuclei (AGNs). A wealth of information gathered through increasingly sophisticated observations over the past three decades has led to a consistent model, in which the fundamental radio emission mechanism is incoherent synchrotron radiation by relativistic particles in a nonuniform magnetic field. The radio and infrared synchrotron photons can inverse Compton (self-Compton) scatter off the radiating particles to produce higher frequency radiation, mostly in the X-ray and gamma-ray range.

The radiating plasma is believed to undergo bulk relativistic motion close to the line of sight. Bulk (or, in some cases, pattern) relativistic motion can provide a simple interpretation of superluminal motion (Rees 1966), rapid flux density variations, deficit of inverse Compton X-rays (Marscher 1987 and references therein) and one-sidedness of jets (Blandford & Königl 1979). Perhaps it could even provide the basis for a unification scheme, in which different types of sources are described as the same intrinsic phenomenon oriented at different angles to the line of sight (for reviews see Blandford 1987; Antonucci 1993).

A fundamental parameter that describes relativistic motion in AGNs is the Doppler factor of the flow,

$$\delta = [\gamma(1 - \beta \cos \varphi)]^{-1} , \quad (1)$$

where β is the speed (in units of the speed of light), $\gamma = (1 - \beta^2)^{-1/2}$ is the Lorentz factor of the flow, and φ is the angle between the direction of the flow and the line of sight. A reliable determination of the Doppler factors for a complete sample of compact radio sources will be of paramount importance for our understanding of the physical processes in these objects.

Ghisellini et al. (1993, hereafter GPCM) took a step in this direction by computing the inverse Compton Doppler factor, δ_{IC} (derived by assuming the observed X-rays to be of inverse Compton origin), for a sample of 105 radio sources with VLBI core size data. They find δ_{IC} to be correlated with other available beaming indicators.

Readhead (1994) suggests another way to estimate the Doppler factor, by assuming the sources to be near equipartition of energy between the radiating particles and magnetic field. The importance and simplicity of the "equipartition Doppler factor," δ_{eq}, lies in the fact that it can be estimated from single-epoch radio data. In addition, δ_{eq}, when compared with another estimate of δ, could provide information about the energetics of the sources (a measure of their departure from equipartition).

Readhead's definition of the equipartition Doppler factor is distinct from that of Singal & Gopal-Krishna (1985), who define an equipartition Doppler factor based on the time variability of the source. Thus, Readhead's equipartition Doppler factor can be estimated from single-epoch radio data, whereas that of Singal & Gopal-Krishna (1985) requires multiepoch radio data.

[1] National Young Investigator.

To examine the question of whether the equipartition Doppler factor (as defined by Readhead 1994) constitutes a reliable estimator of the true Doppler factor δ, δ_{eq} has been computed for the GPCM sample and compared with δ_{IC}.

In §§ 2 and 3 the sample and the formalism used by GPCM to compute δ_{IC} are briefly reviewed. In § 4 the equipartition Doppler factor and the assumptions relevant to the present calculation are discussed. Finally, the results are presented in § 5 and discussed in § 6.

2. THE GPCM SAMPLE

GPCM collected data available from the 1986–1992 literature for all objects with a VLBI-size determination of the radio-emitting core. This gave a total of 105 sources, which were classified into four subgroups: 33 BL Lacertae objects (BLLacs), 53 core-dominated quasars (CDQs), 11 lobe-dominated quasars (LDQs), and eight radio galaxies (RGs). There are enough CDQs for one to further classify them into 24 high-polarization (CDHPQs) and 29 low-polarization quasars (CDLPQs; these actually include seven sources with no polarization data). The sample in general and the criteria for classification are fully discussed by GPCM. It was brought to our attention by the referee that the source 2335+031, which is listed in GPCM as a BLLac, has been shown to have a Seyfert 2–like spectrum (Véron-Cetty & Véron 1993), indicating that it is most probably a narrow-line radio galaxy. In what follows, it is therefore classified as an RG, which brings the total number of RGs up to nine and the number of BLLacs down to 32.

Columns (1)–(6) of Table 1 list the sources in each of the five categories and give the observational data for each source that are relevant to our computation of δ_{eq}: the source redshift z, the frequency of VLBI observation, the flux density and FWHM angular size of the VLBI core [in the case of elliptical Gaussians the value given is $\theta_{FWHM} = (\theta_1\theta_2)^{1/2}$]. In addition, GPCM list the X-ray and optical flux densities, the core-dominance parameter, polarization information, and the fastest apparent transverse speed for all sources for which this information is available. They also list the original references for all the data.

It can be seen in column (3) of Table 1A that six of the BLLacs have lower limits on their redshifts, which are treated as detections, following GPCM. For the five other BLLacs which do not have a redshift determination (see again Table 1A), GPCM have assumed a value $z = 0.4$; the same is done here for the sake of comparison. The redshift value chosen is close to the mean redshift of the remaining BLLacs and gives results consistent with those for the rest of the sample, as is shown below.

TABLE 1A

DATA: BLLacs

Source	Name	z	ν_{obs} (GHz)	S_{obs} (Jy)	θ_{FWHM} (mas)	T_b' (10^{11} K)	T_r (10^{11} K)	δ_{eq}	δ_{IC}	$\frac{\delta_{eq}}{\delta_{IC}}$
(1)	(2)	(3)	(4)	(5)	(6)	(7)	(8)	(9)	(10)	(11)
0048-097	PKS	>0.2	2.3	0.62	0.34	5.5	0.56	12	8.1	1.5
0219+428	3C 66A	0.444	5	0.2	1.5	0.019	1.4	0.02	0.077	0.25
0235+164	AO	0.94	5	1.75	0.5	1.5	0.81	3.7	5.0	0.73
0300+471	4C 47.08	...	22.3	1.1	0.11	1.0	0.77	1.8	3.7	0.49
0306+102	PKS	...	5	0.73	0.5	0.64	0.85	1.0	1.6	0.65
0454+844	S5	>0.3	5	1.3	0.55	0.94	0.81	1.5	2.8	0.53
0537-441	PKS	0.896	2.3	4.2	1.1	3.6	0.76	8.9	8.9	1.0
0716+714	S5	>0.3	5	0.5	0.35	0.89	0.77	1.5	1.6	0.93
0735+178	PKS	>0.424	5	1.29	<0.3	3.1	0.68	6.6	5.6	1.2
0754+100	OJ 090.4	...	5	0.53	0.6	0.32	0.94	0.48	0.85	0.57
0818-128	OJ-131	...	5	0.47	0.8	0.16	1.0	0.21	0.54	0.40
0823+033	0J 038	0.506	15	0.66	<0.1	1.6	0.71	3.4	2.8*	1.2
0829+046	OJ 049	0.18	5	0.26	0.9	0.070	1.1	0.076	0.15	0.50
0851+202	OJ 287	0.306	5	2.3	0.3	5.6	0.62	12	6.8	1.7
0954+658	S4	0.368	5	0.48	0.19	2.9	0.63	6.3	3.8	1.6
1101+384	Mkn 421	0.031	5	0.24	<0.3	0.58	0.61	0.99	0.38	2.6
1147+245	OM 280	>0.2	5	0.39	0.9	0.10	1.1	0.12	0.38	0.31
1215+303	ON 325	...	5	0.33	0.7	0.15	1.0	0.20	0.31	0.64
1219+285	ON 231	0.102	5	0.13	0.5	0.11	0.89	0.14	0.15	0.91
1308+326	B2	0.996	5	1.97	0.5	1.7	0.8	4.3	5.2	0.82
1400+162	4C 16.39	0.244	5	0.08	1.4	0.0089	1.5	0.0075	0.031	0.25
1519-273	PKS	>0.2	2.3	1.59	0.36	13	0.52	29	11*	2.8
1538+149	4C 14.60	0.605	5	0.56	0.6	0.34	0.95	0.57	1.0	0.57
1652+398	Mkn 501	0.034	5	0.45	0.23	1.9	0.53	3.7	1.1	3.2
1727+502	I Zw 186	0.055	5	0.04	1.2	0.0061	1.3	0.0050	0.0077	0.65
1749+096	4C 09.57	0.322	5	1.43	0.2	7.8	0.57	18	11	1.6
1749+701	S5	0.770	5	0.22	0.39	0.31	0.91	0.61	0.85	0.72
1803+784	S5	0.684	5	1.8	0.40	2.5	0.74	5.6	6.6	0.85
1807+698	3C 371	0.051	5	0.95	0.79	0.33	0.78	0.44	0.54	0.83
2007+776	S5	0.342	5	1.17	0.4	1.6	0.74	2.9	3.6	0.80
2200+420	BL Lac	0.069	5	1.6	0.35	2.8	0.58	5.2	3.4	1.5
2254+074	OY 091	0.190	5	0.14	1.0	0.031	1.2	0.030	0.077	0.39

TABLE 1B

DATA: CDHPQs

Source	Name	z	ν_{obs} (GHz)	S_{obs} (Jy)	θ_{FWHM} (mas)	T_b' (10^{11} K)	T_r (10^{11} K)	δ_{eq}	δ_{IC}	$\frac{\delta_{eq}}{\delta_{IC}}$
(1)	(2)	(3)	(4)	(5)	(6)	(7)	(8)	(9)	(10)	(11)
0106+013	4C 01.02	2.107	5	2.30	<0.4	3.1	0.72	14	15	0.93
0133+476	OC 457	0.859	22.3	2.4	0.08	4.1	0.66	12	13*	0.89
0212+735	S5	2.370	5	1.36	0.47	1.3	0.80	5.6	7.1	0.80
0234+285	CTD 20	1.213	22.3	1.7	0.09	2.3	0.72	7.1	13	0.56
0336-019	CTA 26	0.852	2.3	1.52	0.57	4.8	0.67	13	12	1.1
0420-014	PKS	0.915	2.3	3.43	0.70	7.2	0.66	21	13	1.6
0521-365	PKS	0.055	2.3	1.2	1.4	0.63	0.74	0.90	0.77	1.2
0804+499	OJ 508	1.430	5	1.34	0.23	5.5	0.64	21	16	1.3
1034-293	OL-259	0.312	2.3	0.58	0.44	3.1	0.64	6.3	4.2	1.5
1156+295	4C 29.45	0.729	22.2	1.4	<0.123	1.0	0.80	2.2	4.9	0.45
1253-055	3C 279	0.538	15	4.84	0.14	6.0	0.65	14	14	1.0
1335-127	PKS	0.541	2.3	2.21	0.63	5.7	0.66	13	9.2	1.5
1510-089	PKS	0.361	15	2.76	0.12	4.6	0.63	10	11	0.89
1548+056	4C 05.64	1.422	8.4	1.46	0.88	0.15	1.2	0.3	0.69*	0.43
1641+399	3C 345	0.595	22	6.90	0.30	0.86	0.92	1.5	4.1	0.37
1739+522	4C 51.37	1.375	5	0.89	0.37	1.4	0.78	4.3	5.6	0.76
1741-038	OT-68	1.054	2.3	2.11	1.10	1.8	0.82	4.5	3.3*	1.4
1921-293	OV 236	0.352	2.3	3.49	0.54	12	0.58	29	14	2.0
1958-179	PKS	0.65	2.3	1.65	0.52	6.3	0.64	16	7.1*	2.3
2223-052	3C 446	1.404	15	1.98	0.10	4.8	0.65	18	16	1.1
2230+114	CTA 102	1.037	5	0.54	<0.50	0.47	0.91	1	1.5	0.72
2234+282	B2	0.795	5	1.21	<0.50	1.1	0.84	2.3	4	0.57
2251+158	3C 454.4	0.859	5	0.90	<0.30	2.2	0.72	5.6	4.6	1.2
2345-167	PKS	0.576	5	2.50	<0.40	3.4	0.71	7.6	8.3	0.91

The frequencies and flux densities given in columns (4) and (5) of Table 1 are those corresponding to the available VLBI observations, but the formulae for δ_{IC} and δ_{eq} actually require the observed self-absorption turnover frequency ν_{op} and the corresponding peak flux density S_{op} (see §§ 3 and 4). Since their determination requires multifrequency observations and a careful dissection of the observed spectrum to obtain the spectra of the individual components (e.g., Marscher & Broderick 1985; Unwin et al. 1994), these parameters are not yet available for a large sample. GPCM are thus forced to assume that the frequency of observation is the peak frequency; the same assumption is adopted here. All that can be said on its behalf is that real peak frequencies are typically a few giga-

TABLE 1C

DATA: CDLPQs

Source	Name	z	ν_{obs} (GHz)	S_{obs} (Jy)	θ_{FWHM} (mas)	T_b' (10^{11} K)	T_r (10^{11} K)	δ_{eq}	δ_{IC}	$\frac{\delta_{eq}}{\delta_{IC}}$
(1)	(2)	(3)	(4)	(5)	(6)	(7)	(8)	(9)	(10)	(11)
0016+731	S5	1.781	5	1.58	0.46	1.6	0.79	5.7	7.9	0.72
0153+744	S5	2.34	5	0.64	<0.59	0.40	0.94	1.4	1.8	0.80
0229+131	4C 13.14	2.065	8.4	2.76	0.85	0.29	1.1	0.84	2.9	0.29
0333+321	NRAO 140	1.258	3.2	1.60	0.33	7.8	0.62	29	13	2.2
0430+052	3C 120	0.033	5	3.9	<0.4	5.3	0.51	11	4.1	2.7
0528+134	OG 147	2.06	8.4	2.39	0.85	0.26	1.1	0.71	2.0	0.36
0552+398	DA 193	2.365	8.4	2.62	0.73	0.38	1.0	1.2	2.2*	0.58
0615+820	S5	0.71	5	0.61	<0.5	0.53	0.89	1.0	1.5	0.66
0711+356	OI 318	1.620	5	0.27	0.11	4.9	0.58	22	6.4*	3.4
0723-008	OI-039	0.128	2.3	1.07	1.07	0.96	0.75	1.4	1.3	1.1
0836+710	4C 71.07	2.170	5	1.05	0.34	2.0	0.74	8.5	6.7	1.3
0859+470	4C 47.29	1.462	5	1.15	1.40	0.13	1.2	0.26	0.69	0.38
0923+392	4C 39.25	0.699	5	6.9	0.69	3.2	0.78	6.9	8.9	0.77
1039+811	S5	1.26	5	0.29	<0.5	0.25	0.98	0.59	0.69	0.85
1055+201	4C 20.24	1.110	5	0.516	0.2	2.8	0.67	8.9	4.8*	1.9
1150+812	S5	1.25	5	0.46	<0.5	0.4	0.93	0.97	1.5	0.66
1226+023	3C 273	0.158	15	3.49	0.14	4.3	0.61	8.3	4.6	1.8
1404+286	Mkn 668	0.077	8.4	1.05	0.77	0.14	0.95	0.16	0.38	0.4
1548+114	4C 11.50	0.436	5	0.310	0.3	0.75	0.79	1.4	1.4	0.99
1624+416	4C 41.32	2.550	5	0.43	0.33	0.86	0.80	3.8	3.3	1.2
1633+382	4C 38.41	1.814	5	0.43	0.57	0.29	0.98	0.83	2.2	0.39
1730-130	NRAO 530	0.902	15	1.88	0.15	2.0	0.74	5.2	8.5	0.61
1928+738	4C 73.18	0.302	5	2.11	0.49	1.9	0.74	3.4	3.4	0.99
1954+513	OV 591	1.220	5	0.85	1.06	0.17	1.1	0.32	0.54*	0.60
2134+004	PHL 61	1.936	5	6.7	0.62	3.8	0.75	15	27	0.56
2145+067	4C 06.69	0.990	15	5.43	0.16	5.1	0.68	15	21	0.72
2216-038	4C-03.79	0.901	2.3	1.27	0.50	5.2	0.66	15	10	1.5
2245-328	OY-376	2.268	2.3	1.7	1.0	1.8	0.80	7.1	5.1*	1.4
2351+456	4C 45.51	2.000	5	0.32	0.69	0.15	1.1	0.41	0.77	0.53

TABLE 1D

DATA: LDQs

Source	Name	z	ν_{obs} (GHz)	S_{obs} (Jy)	θ_{FWHM} (mas)	T_b' (10^{11} K)	T_r (10^{11} K)	δ_{eq}	δ_{IC}	$\frac{\delta_{eq}}{\delta_{IC}}$
(1)	(2)	(3)	(4)	(5)	(6)	(7)	(8)	(9)	(10)	(11)
0850+581	4C 58.17	1.322	5	0.94	0.48	0.89	0.85	2.4	2.5	0.95
0906+430	3C 216	0.670	5	0.88	0.10	19	0.49	65	33	1.9
1040+123	3C 245	1.029	10.7	0.59	0.33	0.26	0.99	0.53	1.4	0.38
1222+216	4C 21.35	0.435	5	0.691	0.45	0.74	0.83	1.3	1.0*	1.3
1317+520	4C 52.27	1.060	5	0.108	0.8	0.037	1.3	0.060	0.077*	0.77
1618+177	3C 334	0.555	10.7	0.086	<0.2	0.10	1.0	0.16	0.31	0.52
1721+343	4C 34.47	0.2055	10.7	0.109	0.24	0.090	0.96	0.11	0.15	0.73
1830+285	4C 28.45	0.594	5	0.303	0.5	0.26	0.95	0.44	0.38*	1.1
1845+797	3C 390.3	0.057	5	0.31	0.5	0.27	0.76	0.37	0.38	0.98
2209+080	4C 08.64	0.484	5	0.29	3	0.0070	1.8	0.0059	0.023*	0.26
2251+134	4C 13.85	0.677	5	0.37	0.5	0.32	0.94	0.58	0.69*	0.83

hertz, and that the core component dominating at the frequency of observation should be near its peak to account for the observed flat radio spectra of the cores (GPCM).

As indicated in column (6) of Table 1, for 16 sources (three BLLacs, six CDHPQs, five CDLPQs, one LDQ, and one RG) the angular size given is only an upper bound based on the resolution of the VLBI observation. These bounds are treated as detections.

For the computation of δ_{IC} and δ_{eq} one needs the value of the optically thin spectral index α. Following GPCM again, it is assumed here that $\alpha = -0.75$ for all sources (where the flux density $S \propto \nu^{\alpha}$; this is the opposite of the sign-convention adopted by GPCM).

Thirty-five of the 39 sources in the GPCM sample, for which there are transverse speed data from superluminal motion observations, are part of the sample used by Vermeulen & Cohen (1994, hereafter VC), who conducted a thorough study of superluminal motion statistics. (There are 20 sources in VC that are not in GPCM, and 70 sources in GPCM that are not in VC.) As a preamble to their analysis, VC give a careful discussion of the sources in their sample. The four omissions are due to poor determination of their proper motion and thus will not be relevant here. The CDHPQ 2230+114, the CDLPQ 0522+398, and the RGs 0108+388, 0710+439, and 2352+495 are classified by VC as gigahertz-peaked sources, which should not be analyzed together with the other objects. As can be seen below, the inverse Compton and equipartition Doppler factors determined for them are not atypical. VC remark also separately on the CDHPQ 1156+295, which has outstanding optical properties and superluminal speed. Again, this object does not seem peculiar in the context of the present results. The omission of these sources from the following analysis would therefore not affect its main conclusions.

In fact, if a source has both an apparent motion and an estimated Doppler factor, the outflow angle and bulk Lorentz factor may be estimated separately for the source, as discussed by GPCM. Daly, Guerra, & Güijosa (1996) have estimated the outflow angle ϕ and the bulk Lorentz factor γ for several different types of AGN, using the overlap sources from VC and the work presented here. The results are quite interesting; the different categories of AGNs clearly separate out on the ϕ–γ diagram in a way that is consistent with expectations, based on the orientation unified model (Daly, Guerra & Güijosa 1996).

3. INVERSE COMPTON DOPPLER FACTORS

For the simple ideal case of a uniform spherical source of angular diameter θ_d, where the radiating particles have a power-law energy distribution and move in a tangled homogeneous magnetic field (in their rest frame), one can predict the expected inverse Compton X-ray flux density, given the relevant radio and X-ray data. If it is assumed that the emitting material is at rest, the predicted X-ray flux is found in some cases to be many orders of magnitude

TABLE 1E

DATA: RGs

Source	Name	z	ν_{obs} (GHz)	S_{obs} (Jy)	θ_{FWHM} (mas)	T_b' (10^{11} K)	T_r (10^{11} K)	δ_{eq}	δ_{IC}	$\frac{\delta_{eq}}{\delta_{IC}}$
(1)	(2)	(3)	(4)	(5)	(6)	(7)	(8)	(9)	(10)	(11)
0108+388	0C 314	0.669	5	0.56	0.85	0.17	1.1	0.26	0.69	0.38
0316+413	3C 84	0.018	22.2	6	0.30	0.74	0.64	1.2	1.2	0.95
0710+439	S4	0.518	5	0.63	0.96	0.15	1.1	0.21	0.38	0.53
1228+127	M 87	0.004	5	1.0	0.7	0.44	0.53	0.84	0.77	1.1
1637+826	NGC 6251	0.023	10.7	0.67	<0.2	0.80	0.58	1.4	1.0	1.4
2021+614	OW 637	0.227	5	1.01	0.60	0.61	0.84	0.90	1.1*	0.83
2201+044	PKS	0.028	5	0.16	0.70	0.071	0.84	0.087	0.15	0.57
2335+031	4C 03.59	0.31	5	0.03	1.7	0.0023	1.8	0.0017	0.015	0.11
2352+495	OZ 488	0.237	5	0.73	0.82	0.24	0.97	0.30	0.54	0.56

NOTES FOR TABLE 1.—Col. (1), source designation. Col. (2), source name. Col. (3), redshift. Col. (4), frequency of VLBI observation. Col. (5), VLBI flux density. Col. (6), VLBI core FWHM size. Col. (7), observed source brightness temperature. Col. (8) brightness temperature in the source's rest frame (see text). Col. (9), equipartition Doppler factor. Col. (10), inverse Compton Doppler factor (sources marked with an asterisk had no X-ray flux determination, see text). Col. (11), ratio of Doppler factors.

stronger than what is actually observed (e.g., Marscher & Broderick 1981, 1985). This "Compton problem" can be solved by postulating that the source is moving relativistically toward us (Marscher 1987 and references therein). Then the calculation can be turned around to give the value of the Doppler factor that would be needed for the predicted and observed X-ray fluxes to agree (GPCM):

$$\delta_{\rm IC} = f(\alpha) S_m \left[\frac{\ln(\nu_b/\nu_{\rm op}) \nu_{\rm x}^{\alpha}}{S_{\rm x} \theta_d^{6-4\alpha} \nu_{\rm op}^{5-3\alpha}} \right]^{1/(4-2\alpha)} (1+z) , \quad (2)$$

where $S_{\rm x}$ is the observed X-ray flux density (in Jy) at frequency $\nu_{\rm x}$ (keV), $\nu_{\rm op}$ is the observed frequency at the radio peak (in gigahertz), θ_d is the angular diameter of the source (in milliarcseconds), ν_b is the synchrotron high-frequency cutoff (assumed to be 10^5 GHz) and $f(\alpha) \approx -0.08\alpha + 0.14$. The flux density, S_m, that appears (in Jy) in equation (2) is the value that would be obtained at $\nu_{\rm op}$ by extrapolating the optically thin spectrum (Marscher 1987). For $\alpha = -0.75$, this is about a factor of 2 larger than the observed peak flux density $S_{\rm op}$ (Marscher 1977, 1987; see the discussion in § 6). Of course, the formula for $\delta_{\rm IC}$ can be given directly in terms of $S_{\rm op}$ (Cohen 1985), or even in terms of S_n and ν_n, the values at the intersection of the optically thin and thick asymptotes (Unwin et al. 1983). For a uniform sphere the three formulae are equivalent.

The angular diameter of a given component, obtained by modeling it as a sphere, is greater than the observed angular diameter $\theta_{\rm FWHM}$, listed in GPCM and in Table 1. Marscher (1987) suggests correcting for this by using $\theta_d = 1.8\theta_{\rm FWHM}$. By equation (2) this reduces $\delta_{\rm IC}$ by a factor of 2.6 from the values computed by GPCM. This, combined with the increase by a factor of 2 from the use of the extrapolated value of the flux density, leads to a net decrease of the inverse Compton Doppler factors by about a factor of 0.8 from the values obtained by GPCM.

Column (10) of Table 1 lists the values of $\delta_{\rm IC}$, computed by GPCM and multiplied by 0.8 for the reasons given above. For 17 sources without an X-ray data, $\delta_{\rm IC}$ was derived by GPCM using the optical flux (as noted with an asterisk in Table 1). GPCM find that, on average, the values computed this way are underestimated by a factor of about 1.8.

Note that the inverse Compton Doppler factor equals the real Doppler factor δ of the source only if all of the observed X-ray flux is produced through inverse Compton scattering by the component in question. If part of the X-ray flux is produced in other components or by some other mechanism, then $\delta_{\rm IC}$ is a lower limit to δ.

The best determinations of $\delta_{\rm IC}$ to date are those of Marscher & Broderick (1985), who find $\delta_{\rm IC} = 3.7$, for component B of NRAO 140 and, especially, Unwin et al. (1994), who find values of $\delta_{\rm IC} = 7.5$, 1, and 4.6, for components C5, C4, and D of 3C 345, respectively. As already mentioned in § 2, the difficulty of this method lies in the need for multifrequency VLBI observations, a careful dissection of the spectrum to obtain individual component spectra, the identification of any frequency dependence of the angular size, and the avoidance of time-variability effects, by using nearly simultaneous X-ray and radio observations. As a comparison with the above results, note that the values obtained here (Table 1) are $\delta_{\rm IC} = 13$, $\delta_{\rm eq} = 29$ for NRAO 140, and $\delta_{\rm IC} = 4.1$, $\delta_{\rm eq} = 1.5$ for 3C 345.

4. EQUIPARTITION DOPPLER FACTORS

Scott & Readhead (1977) obtain the angular size that a uniform self-absorbed source must have for there to be equipartition of energy between the radiating particles and the magnetic field. This they define as the "equipartition angular size,"

$$\theta_{\rm eq} = 10^3 (2h)^{1/17} F(\alpha) [1 - (1+z)^{-1/2}]^{-1/17} S_p^{8/17} \times (1+z)^{(15-2\alpha)/34} (\nu_p \times 10^3)^{-(2\alpha+35)/34} \text{ mas} , \quad (3a)$$

where the peak flux density S_p and the frequency ν_p have not been corrected for the peculiar motion of the source with respect to the Hubble flow. They are therefore related to the corresponding observed quantities by

$$S_p = \delta^{-3} S_{\rm op} \quad \text{and} \quad \nu_p = \delta^{-1} \nu_{\rm op} , \quad (3b)$$

assuming spherical geometry, where δ is the Doppler factor of the source (eq. [1]). Here and in what follows, flux densities are in janskys, radio frequencies in gigahertz, X-ray frequencies in kilo–electron volts, and angular sizes in milliarcseconds. Equation (3a) has been calculated for an Einstein–de-Sitter cosmology with $H_0 = 100\ h$ km s^{-1} Mpc^{-1}. The equation and a graph for $F(\alpha)$ are given by Scott & Readhead (1977). Here we will only need $F(-0.75) = 3.4$.

The equipartition Doppler-factor (Readhead 1994) is obtained by using equations (3b) in (3a), setting the observed size of the source $\theta_d = \theta_{eq}$, and solving for the Doppler factor. Thus,

$$\delta_{\rm eq} = [[10^3 F(\alpha)]^{34} \{[1 - (1+z)^{-1/2}]/2h\}^{-2} (1+z)^{(15-2\alpha)} \times S_{\rm op}^{16} \theta_d^{-34} (\nu_{\rm op} \times 10^3)^{-(2\alpha+35)}]^{1/(13-2\alpha)} ; \quad (4)$$

note that the entire expression on the right-hand side is raised to the power $1/(13 - 2\alpha)$.

An identical result can be obtained by setting the equipartition brightness temperature $T'_{\rm eq}$ (eq. [4b] in Readhead 1994) equal to the observed brightness temperature of the source at the peak of its spectrum,

$$T'_b = 1.77 \times 10^{12} \frac{S_{\rm op}}{\theta_d^2 \nu_{\rm op}^2} \text{ K} \quad (5)$$

and using equations (3b). (Notice that here, as throughout this paper, $S_{\rm op}$ and $\nu_{\rm op}$ correspond to Readhead's $S'_{\rm op}$ and $\nu'_{\rm op}$. They are the observed peak flux density and frequency for a source at redshift z that has a peculiar motion with respect to the Hubble flow characterized by a Doppler factor δ.)

By definition $\delta_{\rm eq} = \delta$ if $\theta_d = \theta_{\rm eq}$ (or, alternatively, if $T'_b = T'_{\rm eq}$), that is, $\delta_{\rm eq} = \delta$ if the source is at equipartition. Otherwise, the ratio $\delta_{\rm eq}/\delta = T'_b/T'_{\rm eq}$ is a measure of the source's departure from equipartition; it determines the ratio of the particle and magnetic energy densities u_p and u_m. For instance, in an electron-positron plasma (Readhead 1994),

$$\frac{u_p}{u_m} = \left(\frac{\delta_{\rm eq}}{\delta} \right)^{17/2} . \quad (6)$$

Readhead (1994) shows that the distribution of brightness temperatures for powerful radio sources has its upper cutoff at $\sim 10^{11}$ K, well below the value at which the inverse Compton catastrophe (the rapid loss of energy through inverse Compton scattering) can operate. He points out that the equipartition brightness temperature is typically

TABLE 2

MEAN VALUES: ALL SOURCES

Class	N	δ_{eq}		δ_{IC}		δ_{eq}/δ_{IC}	
		Mean	Range	Mean	Range	Mean	Range
All Sources	105	5.8 ± 0.9	0.0017-65	4.8 ± 0.6	0.0077-33	1.0 ± 0.1	0.11-3.4
BL Lacs	32	4.1 ± 1.1	0.0050-29	3.1 ± 0.6	0.0077-11	1.0 ± 0.1	0.24-3.2
CDQs	53	7.7 ± 1.0	0.16-29	6.7 ± 0.8	0.38-27	1.1 ± 0.1	0.29-3.4
CDHPQs	24	9.6 ± 1.5	0.30-29	8.4 ± 1.0	0.69-16	1.1 ± 0.1	0.37-2.3
CDLPQs	29	6.1 ± 1.3	0.16-29	5.3 ± 1.1	0.38-27	1.0 ± 0.1	0.29-3.4
LDQs	11	6.4 ± 5.9	0.0059-65	3.7 ± 3.0	0.023-33	0.89 ± 0.14	0.26-1.9
LDQs -1	10	0.60 ± 0.23	0.0059-2.4	0.70 ± 0.25	0.023-2.5	0.78 ± 0.10	0.26-1.3
RGs	9	0.51 ± 0.17	0.0017-1.4	0.65 ± 0.14	0.015-1.2	0.71 ± 0.13	0.11-1.4

$\sim 10^{11}$ K, and is therefore a more accurate cutoff. Readhead's conclusion is that the upper limit for T_b' in the radio emission regions is given by some mechanism which prevents significant departures from equipartition.

Column (9) of Table 1 lists the equipartition Doppler factors (eq. [4]) for the GPCM sample. We have assumed $h = 1$, $S_{op} = S_{obs}$, $\nu_{op} = \nu_{obs}$, and $\theta_d = 1.8\theta_{FWHM}$ (see § 3). For reference, column (7) of Table 1 gives the observed brightness temperatures T_b' computed with equation (5) (notice this is not the same as GPCMs eq. [5], which has an additional factor of $1 + z$). Finally, column (8) lists the corresponding intrinsic brightness temperatures in the sources' rest frame, $T_r = T_b'(1 + z)/\delta$, calculated assuming $\delta = \delta_{eq}$.

5. RESULTS

The ratio δ_{eq}/δ_{IC} is listed for each source in column (11) of Table 1. The mean value, standard deviation of the mean, and range of these ratios, as well as of the individual Doppler factors for each class of source and the entire sample, are given in Table 2. Due to the exceptionally large values of δ_{eq} and δ_{IC} for the LDQ 3C 216 (65 and 33, respectively; see Table 1D), the statistical information for the LDQs is given in Table 2, both with and without this source; the latter class of sources is referred to as LDQs − 1. It is evident from Table 2 that the mean ratio of Doppler factors, δ_{eq}/δ_{IC}, estimated as described above, is on the order of unity.

Plots of δ_{eq} versus δ_{IC} for the entire sample, and for each subsample separately, are shown in Figures 1*a*–1*f*. The high correlation of δ_{eq} and δ_{IC} is apparent. Figures 1*a*–1*f* also show for each case the best-fitting (unweighted) line for δ_{eq} versus δ_{IC} that passes through the origin. The best-fitting slopes and their 1 σ errors are given in Table 3. Best-fitting lines allowed to have nonzero intercepts have also been calculated. The resulting intercepts and slopes along with their 1 σ errors are listed in Table 3. It can be seen in Figure 1*f* that the LDQ 3C 216 is outstanding, even relative to the entire sample. The regression parameters have therefore been computed also for the sample with this source omitted (this is referred to as All − 1 in Table 3). Note, however, that this source is not totally unusual in terms of its distance from the best-fitting line or its value of δ_{eq}/δ_{IC}.

A log–log plot of δ_{eq} versus δ_{IC} for the entire sample is given in Figure 2, together with a linear fit in the log–log plane, $\log \delta_{eq} = a \log \delta_{IC} + b$. The best fitting parameters are $a = 1.2 \pm 0.03$, $b = -0.13 \pm 0.02$. The slight offset of the slope from unity might imply jetlike rather than spherical geometry (see § 6).

The statistical errors taken into account for the intervals in Table 3 are just those given by the linear regression formalism in terms of the scatter of the points about the regression line. At present a detailed calculation of statistical errors for each δ_{eq} and δ_{IC} is unwarranted. Most of the error comes from θ_d and, especially, from the unknown ν_{op}. The uncertainly in the peak frequency is probably at least 100% (e.g., GPCM take a value of 22 GHz for 3C 345; but Unwin et al. 1994 find a turnover frequency of ~ 3 GHz for its component C5). As can be seen from equation (4), $\delta_{eq} \propto \nu_{op}^{-(35+2\alpha)/(13-2\alpha)}\theta_d^{-34/(13-2\alpha)}$. For $\alpha = -0.75$ this is $\delta_{eq} \propto \nu_{op}^{-2.3}\theta_d^{-2.3}$. Thus we have for δ_{eq} a minimal uncertainty of about 200%. Similarly, from equation (2) the uncertainty in δ_{IC} is at least $\sim 100\%$.

Since the dependence of δ_{eq} and δ_{IC} on the observables is similar, it is clear that their ratio can be determined more precisely than their individual values. Indeed, for $\alpha = -0.75$ we have $\delta_{eq}/\delta_{IC} \propto \nu_{op}^{-1.0}\theta_d^{-0.7}$.

The dependence of δ_{eq}/δ_{IC} on redshift for the entire sample is shown in Figure 3, along with the corresponding

TABLE 3

REGRESSION SLOPES FOR δ_{eq} VERSUS δ_{IC}: ALL SOURCES

Class	N	Zero Intercept	Non-zero Intercept	
		Slope	Slope	Intercept
All Sources	105	1.3 ± 0.1	1.3 ± 0.1	-0.48 ± 0.59
All -1	104	1.1 ± 0.1	1.1 ± 0.1	0.33 ± 0.53
BL Lacs	32	1.5 ± 0.1	1.7 ± 0.2	-1.1 ± 0.7
CDHPQs	24	1.2 ± 0.1	1.2 ± 0.2	-0.94 ± 1.7
CDLPQs	29	0.96 ± 0.12	0.82 ± 0.16	1.7 ± 1.3
LDQs	11	1.9 ± 0.03	2.0 ± 0.03	-0.75 ± 0.29
LDQs -1	10	0.87 ± 0.09	0.88 ± 0.13	-0.018 ± 0.13
RGs	9	0.94 ± 0.11	1.1 ± 0.2	-0.14 ± 0.16
All (log-log)	105	...	1.2 ± 0.03	-0.13 ± 0.02

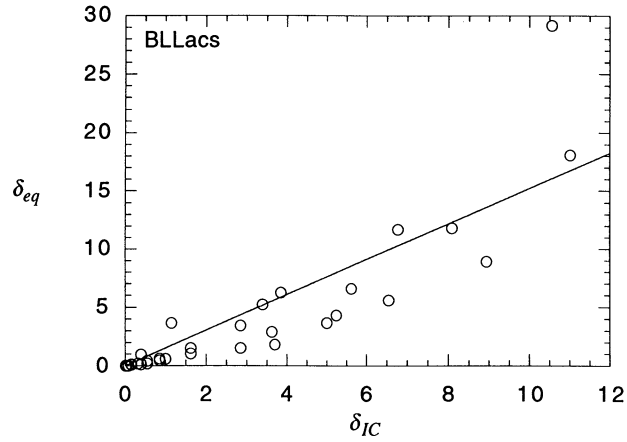

FIG. 1*a*

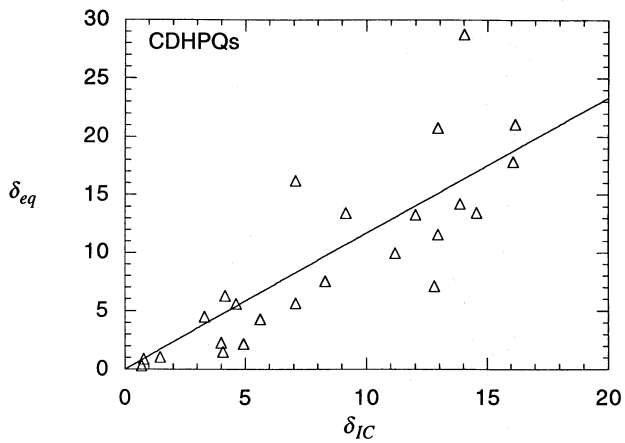

FIG. 1*b*

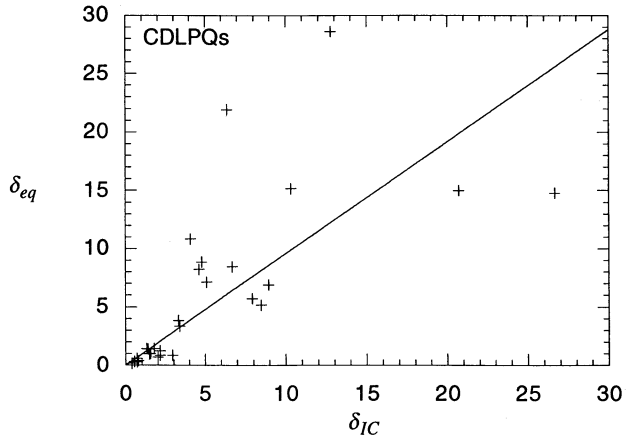

FIG. 1*c*

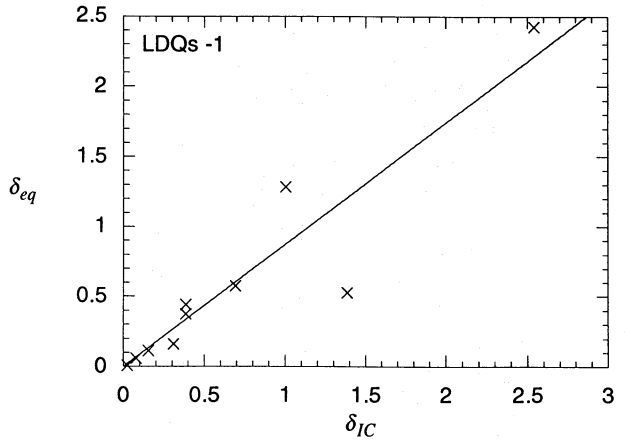

FIG. 1*d*

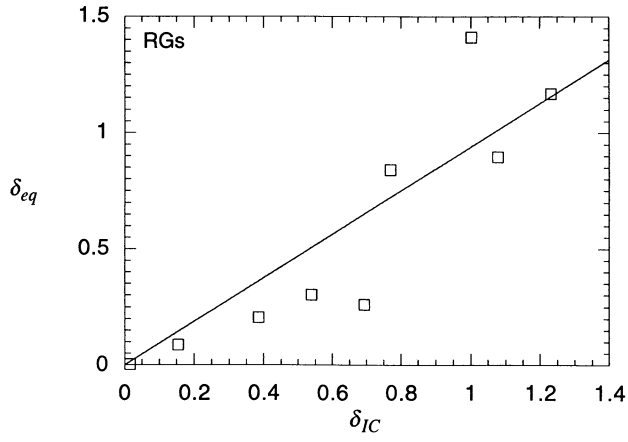

FIG. 1*e*

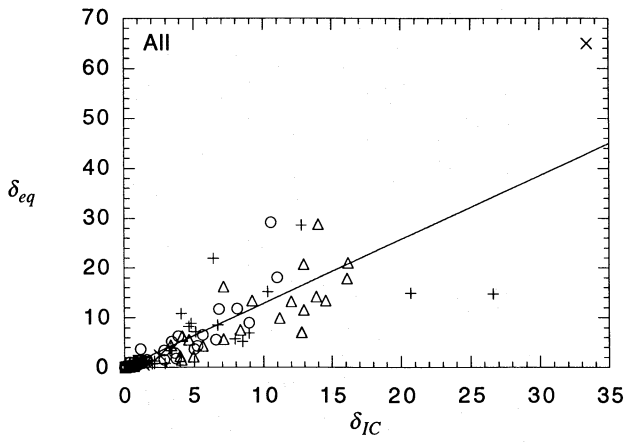

FIG. 1*f*

FIG. 1.—Equipartition versus inverse Compton Doppler factors for: (*a*) BLLacs (*circles*), (*b*) CDHPQs (*triangles*), (*c*) CDLPQSs (*crosses*), (*d*) LQDs −1 (*rotated crosses*), (*e*) *RGs* (*squares*), and (*f*) entire sample (*linear scale*). Also shown in each case are best-fitting lines through the origin (see text). The corresponding regression parameters are given in Table 3.

linear fit. The slope of the best-fitting line and its 1 σ interval is -0.12 ± 0.09. The slopes of the best-fitting lines in the δ_{eq}/δ_{IC} versus $1 + z$ plots for the individual subsamples are: -0.87 ± 0.48 (BLLacs), -0.27 ± 0.18 (CDHPQs), -0.20 ± 0.18 (CDLPQs), -0.10 ± 0.29 (LDQs −1), and -1.1 ± 0.5 (RGs). Thus, at the 1–2 σ level, the Doppler factor ratios of the sources appear to be independent of redshift.

There also appears to be no systematic dependence of δ_{eq}/δ_{IC} on the observed luminosity. This is manifest in Figure 4, which shows the logarithm of the ratio of Doppler factors as a function of log L_{obs}. The observed monochromatic luminosities have been computed using the monochromatic luminosity distance (Von Hoerner 1974), with cosmological parameters $h = 1$ and $q_0 = 0.5$. It must be born in mind that these luminosities correspond to different frequencies, and that no correction has been made for the relativistic boosting to obtain rest-frame luminosities.

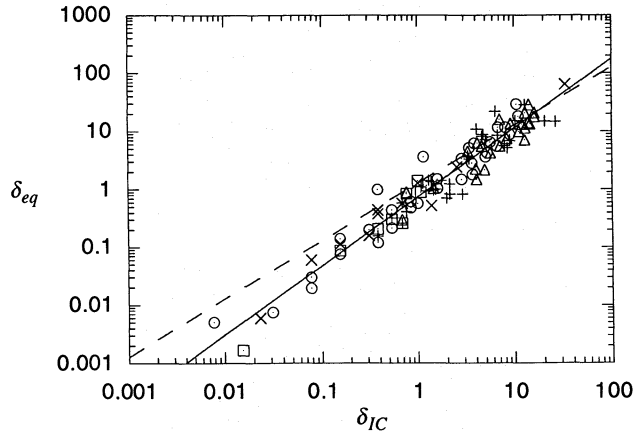

FIG. 2.—Equipartition versus inverse Compton Doppler factors for the entire sample (log-log scale). The symbols are as in Figs. 1*a*–1*f*. The solid line is the best-fitting line in the log-log plane (see text); the dashed line is the best-fitting line from Fig. 1*f*.

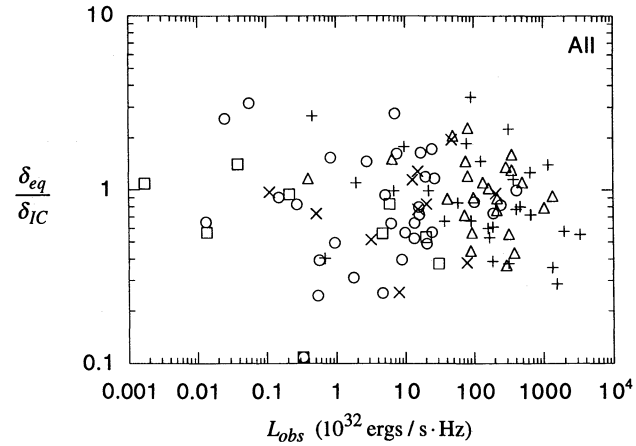

FIG. 4.—Ratio of Doppler factors δ_{eq}/δ_{IC} vs. observed monochromatic luminosity (log-log scale) for BLLacs (*circles*), CDHPQs (*triangles*), CDLPQs (*crosses*), LDQs (*rotated crosses*), and RGs (*squares*).

6. DISCUSSION

Several conclusions can be drawn from the results presented in § 5. First and most important, a high correlation is found between the two totally independent estimates of the Doppler factor (better than 99% for BLLacs, CDHPQs, CDLPQs, LDQs, RGs, and the entire sample). As a result of this, δ_{eq} is also expected to be highly correlated with the beaming factors that GPCM find to be correlated with δ_{IC}. Second, the points (δ_{IC}, δ_{eq}) are clearly scattered close to the $\delta_{eq} = \delta_{IC}$ line. These two results seem to indicate that both δ_{eq} and δ_{IC} may be reliable estimators of the true Doppler factor δ.

One worry is that although it seems that $\delta_{eq} \approx \delta_{IC}$, it could be that neither is truly a good estimate of δ. The high correlations found between δ_{eq} and δ_{IC} could simply be due to their similar dependence on the observed quantities. It is shown below that this is probably not the case, and this point is under more detailed investigation (Guerra & Daly 1996).

From equations (2) and (4) it can be seen that (for $\alpha = -0.75$), the dependence of the ratio of Doppler factors on observables is roughly

$$\frac{\delta_{eq}}{\delta_{IC}} \propto \{[(1+z) - (1+z)^{0.5}] S_{op}\, \nu_x\}^{0.1} S_x^{0.2} \theta_d^{-0.7} \nu_{op}^{-1.0} \,. \quad (7)$$

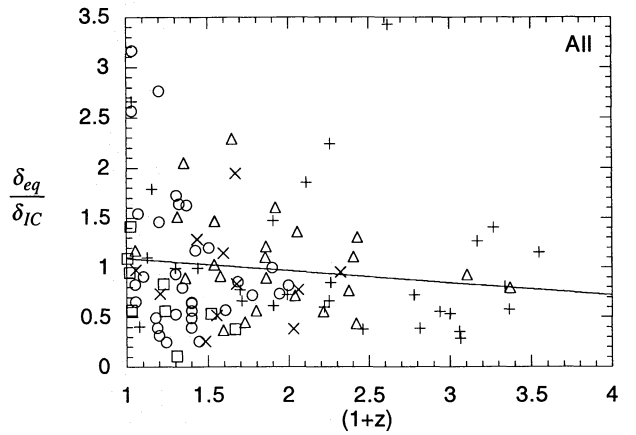

FIG. 3.—Ratio of Doppler factors δ_{eq}/δ_{IC} vs. $1 + z$ for the entire sample: BLLacs (*circles*), CDHPQs (*triangles*), CDLPQs (*crosses*), LDQs (*rotated crosses*), and RGs (*squares*). Also shown is the best-fitting line (see text).

For the range of the variables in the sample (see Table 1 and GPCM) this ratio could vary by as much as 3 orders of magnitude. Since the actual ratios vary by only 1 order of magnitude, it seems that the observable quantities are, for physical reasons, related in such a way as to make the ratios approximately constant. Hence, it does indeed appear to be the case that the correlation between the Doppler factors is physical in origin, and that $\delta_{eq} = \delta_{IC} \approx \delta$.

Different assumptions about the geometry of the sources will lead to different conclusions about the relation between the estimated Doppler factors. There are two distinct reasons for this. First, the formulae for the Doppler factors are certainly geometry dependent. Consider, for instance, the case of jetlike rather than spherical structure. For the jet case, GPCM show that $\delta_{IC,jet} = \delta_{IC,sphere}^{(4-2\alpha)/(3-2\alpha)}$. Thus, for $\alpha = -0.75$ the derived inverse Compton Doppler factors are higher (lower) for jets than for spheres if $\delta > 1$ ($\delta < 1$). Similarly, the formula for the equipartition Doppler factor of a jet is expected to be slightly different from that of a sphere. A jetlike model could perhaps account for the slight offset of the log δ_{eq} versus log δ_{IC} line (Fig. 2) from unit slope.

Second, assumptions about the geometry of the sources are related to the way observational data are substituted into the formulae (eqs. [2] and [4]). In § 3, following Marscher (1977, 1987), the angular size of the sources was corrected by a factor of 1.8, and a value of 2.0 was adopted for the ratio $r \equiv S_m/S_{op}$ of the extrapolated flux density at the peak, S_m, to the observed peak flux density, S_{op}, using $r = \exp \tau$, where the optical depth at the peak is $\tau = 0.69$, for $\alpha = -0.75$. The formulae of Marscher are derived using a self-consistent model of inhomogeneities within the source. In the simple homogeneous spherical geometry of Gould (1979), and the slab geometry discussed in the appendix of Scott & Readhead (1977), it is found that $r \approx 1.3$. If this value is used instead of $r \approx 2.0$, the values of δ_{IC} decrease by a factor of about 1.6 from those given in Table 1. Thus, the ratios of Doppler factors are sensitive to the value of r adopted, even though at the (rather low) present level of accuracy it is not possible to discriminate between different values of r. (In particular, it should be remembered that at this stage the true observed peak flux densities of the sources are unavailable.) In any case, it should be clear that the consistency of the highly idealized assumptions for the geometry of the models employed can be tested with a more

precise set of data. More complex models will require more data to constrain them; for example, Unwin et al. (1994) have been able to use a conical jet model for the nucleus (component D) of 3C 345.

One must remember that $\delta_{IC} = \delta$ only if the component in question is the sole source of the observed X-ray flux, and if this flux is entirely of inverse Compton origin. Otherwise, $\delta > \delta_{IC}$. (For instance, even in the more precise calculation of Unwin et al. 1994 it is clear that their derived values for the inverse Compton Doppler factor of components C5, C4, and D cannot all be equal to the true Doppler factors, since each one is derived using the total X-ray flux from 3C 345.)

Note also that $\delta = \delta_{eq}$ only if the component in question is at equipartition. Otherwise, if the average ratio δ_{eq}/δ were known, equation (6) could be used (assuming an electron–positron plasma) to estimate the typical ratio of energies u_p/u_m. However, because of the strong dependence of u_p/u_m on δ_{eq}/δ, the uncertainty of this estimate can be high. In the present case, it is assumed that the standard deviation of δ_{eq}/δ is of the order of that for δ_{eq}/δ_{IC}, then the uncertainty in the mean ratio of Doppler factors of $\sim 10\%$ (Table 2) renders the mean value of u_p/u_m uncertain by $\sim 100\%$. Thus, our results are consistent with the sources having energy densities fairly close to their equipartition values.

The mean Doppler factor ratios (Table 2) and the regression slope values (Table 3) of the separate subsamples are all consistent at the 1 σ or 2 σ level. This is rather remarkable given the potentially large systematic errors and the simplifying model assumptions. It will be very interesting to see whether this remains true when a larger and more precise data set is available.

It is interesting that the Doppler factors estimated for RGs and LDQs -1 are on average below unity, while those of other classes of sources are larger than unity. This suggests that RGs and LDQs lie much closer to the plane of the sky, that is, have smaller values of cos φ, than the other types of sources, as discussed, for example, by GPCM. It is not clear whether this is related to the corresponding low values of δ_{eq}/δ_{IC}. Any discrepancies among the mean values of this ratio of Doppler factors or among the mean values of the two estimates of the Doppler factors for different classes of sources could, perhaps, be used to support or reject the proposed orientation unified schemes.

Obviously, it is important to determine the ratios of equipartition and inverse Compton Doppler factors for a complete sample of radio sources using careful observations and theoretical considerations. If a firm value of δ_{eq}/δ_{IC} can be established statistically (be it for the entire sample or separately for each category), then, as Unwin et al. (1994) have pointed out, the Doppler factor could be estimated from single-epoch radio data. In addition, the results presented here suggest that equipartition Doppler factors alone could provide a useful estimate of the true Doppler factors. This in turn would allow the X-ray flux densities to be reliable predicted. Thus, the equipartition Doppler factor will, in all likelihood, play a crucial role in our understanding of the physics at work in compact radio sources.

It is a pleasure to thank Marshall Cohen, Ken Kellermann, Alan Marscher, the referee Paolo Padovani, Tim Pearson, Tony Readhead, Larry Rudnick, and Peter Scheuer for stimulating discussions and useful comments regarding this paper. This work was supported in part by the US National Science Foundation and the Independent College Fund of New Jersey.

REFERENCES

Antonucci, R. 1993, ARA&A, 473
Blandford, R. D. 1987, in Superluminal Radio Sources, ed. J. A. Zensus & T. J. Pearson (Cambridge: Cambridge Univ. Press), 310
Blandford, R. D., & Königl, A. 1979, ApJ, 232, 34
Cohen, M. H. 1985, in Extragalactic Energetic Sources, ed. V. K. Kapahi (Bangalore: Indian Acad. Sci), 1
Daly, R. A., Guerra, E. J., & Güijosa, A. 1996, in Energy Transport in Radio Galaxies and Quasars, ed. P. Hardee, A. Bridle, & A. Zensus (ASP Conf. Series), in press
Ghisellini, G., Padovani, P., Celotti, A., & Maraschi, L. 1993, ApJ, 407, 65
Gould, R. J. 1979, A&A, 76, 306
Guerra, E. J., & Daly, R. A. 1996, ApJ, in preparation
Marscher, A. P. 1977, ApJ, 216, 244
———. 1987, in Superluminal Radio Sources, ed. J. A. Zensus & T. J. Pearson (Cambridge: Cambridge Univ. Press), 280
Marscher, A. P., & Broderick, J. J. 1981, ApJ, 249, 406
———. 1985, ApJ, 290, 735
Readhead, A. C. S. 1994, ApJ, 426, 51
Rees, M. J. 1966, Nature, 211, 468
Scott, M. A., & Readhead, A. C. S. 1977, MNRAS, 180, 539
Singal, A. K., & Gopal-Krishna 1985, MNRAS, 215, 383
Unwin, S. C., Cohen, M. H., Pearson, T. J., Seielstad, G. A., Simon, R. S., Linfield, R. P., & Walker, R. C. 1983, ApJ, 271, 536
Unwin, S. C., Wehrle, A. E., Urry, C. M., Gilmore, D. M., Barton, E. J., Kjerulf, B. C., Zensus, J. A., & Rabaca, C. R. 1994, ApJ, 432, 103
Vermeulen, R. C., & Cohen, M. H. 1994, ApJ, 430, 467
Véron-Cetty, M. P., & Véron, P. 1993, A&AS, 100, 521
Von Hoerner, S. 1974, in Galactic and Extragalactic Radio Astronomy, ed. G. L. Verschuur & K. I. Kellerman (New York: Springer), 353